

## Reentrance Effect in Macroscopic Quantum Tunneling and Nonadiabatic Josephson Dynamics in $d$ -Wave Junctions

J. Michelsen and V. S. Shumeiko

*Department of Microtechnology and Nanoscience, MC2, Chalmers University of Technology, SE-41296 Gothenburg, Sweden*  
(Received 7 May 2010; published 16 September 2010)

We develop a theoretical description of nonadiabatic Josephson dynamics in superconducting junctions containing low energy quasiparticles. Within this approach we investigate the effects of midgap states in junctions of unconventional  $d$ -wave superconductors. We identify a reentrance effect in the transition between thermal activation and macroscopic quantum tunneling, and connect this phenomenon to the experimental observations in *Phys. Rev. Lett.* **94**, 087003 (2005). It is also shown that nonlinear Josephson dynamics can be defined by resonant interaction with midgap states reminiscent of nonlinear optical phenomena in media of two-level atoms.

DOI: [10.1103/PhysRevLett.105.127001](https://doi.org/10.1103/PhysRevLett.105.127001)

PACS numbers: 74.50.+r, 74.40.Gh, 74.45.+c, 74.72.-h

With the advent of superconducting qubits [1–3] a general interest has grown towards realization of macroscopic quantum dynamics in superconducting weak links. The superconducting qubits developed so far are based on Josephson tunnel junctions of conventional superconductors. A conceptually interesting and practically important question is whether other types of Josephson weak links, such as junctions of high temperature superconductors, and mesoscopic metallic or semiconducting weak links can be employed in qubit circuits. The central aspect of this problem is to understand the role of low energy electronic states usually present in such junctions. The low energy quasiparticles are driven away from equilibrium by temporal variation of the superconducting phase across the junction and produce a nonadiabatic contribution to the Josephson current. This effect is commonly considered to result in dissipation and decoherence of qubit states. However, examples from nonlinear optics show that resonant interaction with *localized* electronic states (two-level atoms) may generate a nonlinear dispersion of electromagnetic modes leading to a variety of nonlinear phenomena involving coherent energy exchange between macroscopic and microscopic variables [4]. This kind of nonlinear phenomena, whose origin differs from the nonlinearity of the adiabatic Josephson potential, has never been studied in the context of macroscopic Josephson dynamics.

In this Letter we investigate the nonadiabatic Josephson dynamics in artificial grain boundary junctions of high temperature superconductors [5], which is caused by interaction with superconducting surface bound states [midgap states (MGS)]. The MGS situate at zero energy in the middle of the superconducting energy gap [6] and are fundamentally connected to the unconventional  $d$ -wave superconducting order parameter in these materials [7,8]. We find that interaction with the MGS has implications in both the imaginary time dynamics (tunneling) and the real time nonlinear dynamics of the junction. First, we show that the MGS are capable of significantly affecting the transition between the thermal activation and macroscopic

quantum tunneling (MQT) decay of Josephson current state inducing multiple, forward and backward, transitions between the two regimes. We suggest that such a reentrance phenomenon underlines the experimentally observed [9] anomaly of the switching current rates. Secondly, we show that the nonlinear resonant response of  $d$ -wave junctions may be entirely caused by the nonlinear dynamics of the MGS and lead to a bifurcation regime with an explosive growth of the response amplitude. These findings are made within the framework of a general theoretical description of the nonadiabatic Josephson dynamics in junctions containing low energy quasiparticles developed in this Letter.

The special role of the MGS is explained by their discrete energy spectrum and pairwise coupling to the temporal variation of the superconducting phase. Tunneling spectroscopy data [10] as well as observation of a  $\pi$ -junction transition [11] provide experimental evidence for the MGS existence. The equilibrium properties of MGS and their role in the dc Josephson effect are well studied in the literature (see reviews [12,13] and references therein). The multiple degenerate zero energy level of the MGS splits into a narrow band under the effects of tunneling and anisotropy of the  $d$ -wave order parameter,  $\Delta(\mathbf{k}_F) = \Delta_0 \cos(2\theta)$ . Because of the small bandwidth a thermal saturation of the MGS occurs at relatively low temperatures that may be comparable to the MQT transition temperature. This saturation effect accompanied by the decrease of the MGS-induced dissipation underlines, as we show, the reentrance effect in the MQT transition. In junctions with atomically smooth interfaces, a large fraction of tunneling electron trajectories contains hybridized MGS pairs. The two-state Rabi dynamics and the MGS saturation at large driving amplitudes define the nonlinear property of real time Josephson dynamics.

*MQT transition temperature.*—We start with the discussion of the effect of MGS on the MQT transition temperature. We follow the method of Ref. [14], based on the analysis of the imaginary time dynamics of phase fluctua-

tions,  $\delta\varphi(\tau)$ , around the steady phase difference across the junction,  $\varphi = \varphi_b$ , at the top of the barrier of the tilted Josephson potential. In this method, the MQT transition is manifested by an instability of the phase fluctuations described with an effective Euclidian action,  $S_{\text{eff}}[\varphi] \approx S_{\text{eff}}[\varphi_b] + \sum_n \Lambda(\varphi_b, i\nu_n) \delta\varphi_n \delta\varphi_{-n}$ ,  $\nu_n = 2\pi nT$  ( $k_B = \hbar = 1$ ). The transition corresponds to the change of the sign of the kernel,  $\Lambda(\varphi_b, i\nu_1)$ , and the temperature is given by the equation  $\Lambda(\varphi_b, i\nu_1) = 0$ .

To derive the effective action for the superconducting phase, we consider the partition function of  $d$ -wave junction,  $Z = \int \mathcal{D}\varphi \mathcal{D}^2\psi e^{-(S_\varphi[\varphi] + S_\psi[\varphi, \psi])}$ , and perform integration over fermionic variables  $\psi$  [15]. Here,  $S_\varphi = \int d\tau [(C/8e^2)\dot{\varphi}^2 - I_e\varphi/2e]$  is the macroscopic part of the action contributed by the charging energy of the junction capacitance  $C$  and the inductive energy of the biasing current  $I_e$ . Furthermore,  $S_\psi = \int d\tau \int dr \bar{\psi} [\partial_\tau + \mathcal{H} + (i/4)\text{sgn}(x)\dot{\varphi}]\psi$  is the microscopic part of the action, associated with the mean-field Hamiltonian of the superconducting electrons  $\mathcal{H}$ , where the last term provides electroneutrality within the electrodes [16].

We perform the integration by choosing a general method suitable for all kinds of junctions regardless of their transparencies or presence of localized surface states. We separate the spatial problem from the temporal one by introducing a basis of *instantaneous* eigenstates of electronic Hamiltonian,  $\mathcal{H}\phi_i = E_i\phi_i$ ,  $\psi(\mathbf{r}, \tau) = \sum_i \phi_i(\mathbf{r}; \varphi) a_i(\tau)$ . The fermionic action then becomes  $S_\psi = \int d\tau \sum_{ij} \bar{a}_i G_{ij}^{-1} a_j$ , where  $G_{ij}^{-1} = \partial_\tau + H_{ij}(\varphi, \dot{\varphi})$  is the inverse Green function of the effective Hamiltonian,

$$H_{ij} = E_i \delta_{ij} - i\dot{\varphi} \mathcal{A}_{ij}; \quad (1)$$

$$\mathcal{A}_{ij} = (\phi_i, i\partial_\varphi \phi_j) - (1/4)(\phi_i, \text{sgn}(x)\sigma_z \phi_j) \quad (2)$$

is the matrix element of quasiparticle transitions induced by temporal variation of the phase. The effective action has the form  $S_{\text{eff}}[\varphi] = S_\varphi - \text{Sp} \ln \hat{G}^{-1}$ .

The saddle point solution is given by the equation  $\delta S_{\text{eff}} = 0$ . For the fermionic contribution we have  $\delta \text{Sp} \ln \hat{G}^{-1} = (1/2e) \text{Sp}(\hat{I}_J \hat{G} \delta\varphi)$ , where

$$\hat{I}_J = 2e(\partial_\varphi \hat{E} + i[\hat{E}, \hat{\mathcal{A}}]) \quad (3)$$

is the Josephson current operator [16,17]. At the static saddle point,  $-\hat{G}^0(\tau, \tau) = \hat{n}^0(\hat{E})$  is the equilibrium density matrix commuting with  $\hat{E}$ ; therefore, only the diagonal (adiabatic) part of the current operator contributes to the Josephson current,  $I_J^d(\varphi) = 2e \sum_i \partial_\varphi E_i n_i^0$ , that defines  $\varphi_b$ ,  $I_J^d(\varphi_b) - I_e = 0$ .

The nonadiabatic effect is described by the second functional derivative of the fermionic action,  $(1/2e)^2 \text{Sp}(\delta\varphi \hat{I}_J \hat{G}^0 \hat{I}_J \hat{G}^0 \delta\varphi)$ , and the fluctuation kernel reads [17]  $\Lambda(i\nu_n) = (C/8e^2)[\nu_n^2 - \omega_b^2 - i\nu_n \gamma_0(i\nu_n)]$ . Here,  $\omega_b^2 = -(2e/C)\partial_\varphi I_J^d$  is the plasma frequency at the barrier and

$$\gamma_0(i\nu_n) = \frac{4e^2}{C} \sum_{ij} \frac{\varepsilon_{ij} |\mathcal{A}_{ij}|^2 (n_i^0 - n_j^0)}{\varepsilon_{ij} - i\nu_n} \quad (4)$$

is the quasiparticle response;  $\varepsilon_{ij} = E_i - E_j$ ,  $n_i^0 = n_F(E_i)$  is the Fermi filling factor, all functions are taken at  $\varphi = \varphi_b$ .

Up to this point the derivation is general, and Eq. (4) applies to all the quasiparticles. At small frequencies, however, only the MGS and itinerant nodal quasiparticles [18] are relevant. Furthermore, the MGS contribution has more pronounced temperature dependence compared to the nodal states because MGS have a small bandwidth,  $\varepsilon_m \ll \Delta_0$ . Focusing on the more interesting effect of the MGS, we truncate Eq. (4) to the MGS subspace. The matrix elements  $\mathcal{A}_{ij}$  only connect MGS pairs of the same electronic trajectory while transitions among the trajectories are forbidden due to preserved translational invariance. Parametrizing the MGS pairs with the angle  $\theta$  between the incidental wave vector  $\mathbf{k}_F$  of the respective trajectory and the interface normal (see top inset Fig. 1), and denoting,  $\varepsilon(\theta) = E_1(\theta) - E_2(\theta)$ ,  $A(\theta) = \mathcal{A}_{12}$ , we present the equation for the transition temperature on the form

$$\nu^2 - \omega_b^2 - \frac{8e^2 S}{C} \nu^2 \left\langle \frac{\varepsilon A^2 (n_1^0 - n_2^0)}{\varepsilon^2 + \nu^2} \right\rangle = 0, \quad (5)$$

where angle brackets indicate the average over the Fermi surface,  $S$  is the junction area,  $\nu = 2\pi T$ .

The temperature dispersion of the MGS term in Eq. (5) is primarily defined by the Fermi filling factors and the resonant denominator, while the particular form of the smooth functions  $\varepsilon(\theta)$  and  $A(\theta)$  plays a secondary role. This allows us to formulate an *analytical* model equation

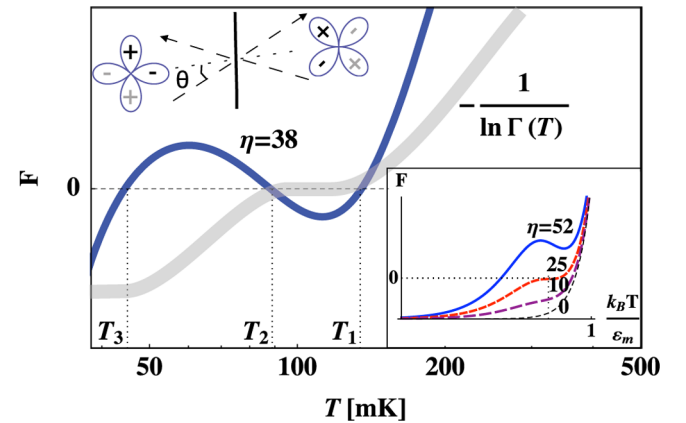


FIG. 1 (color online). Reentrance effect in MQT. Sketch of temperature dependence of decay rate (wide shadow line) illustrates the effect featuring three transitions between thermal activation and MQT regimes. Experimental transition temperatures are given by zeros of function  $F(x)$ , defined in the text [dark gray (blue) line] for  $\eta = 38$ . Lower inset shows development of nonmonotonic feature of function  $F(x)$  with increasing  $\eta$ , at  $\eta > 25$ . Upper inset illustrates junction geometry and scattering electron trajectory (dashed line).

for the transition temperature, thus circumventing the difficulty of evaluating anisotropy of the MGS, which generally can only be done numerically. By replacing  $\varepsilon A^2(\theta)(d\varepsilon/d\theta)^{-1}$  with a constant, we get Eq. (5) on the form  $F(x) = \varepsilon_m^2 x^2 [1 + \eta f(x)] - \omega_b^2 = 0$ , where  $f(x) = \int_0^1 dy \tanh(\pi y/2x)(x^2 + y^2)^{-1}$ , and  $x = \nu/\varepsilon_m$ ;  $\eta = 8a\pi/R_n C \varepsilon_m$  is the coupling strength,  $R_n = \pi/e^2 S \langle D \rangle$  is the normal junction resistance, and  $a \sim 1$  is a geometry specific constant. The latter estimate is obtained from the scaling,  $\varepsilon_m \propto \sqrt{D} \Delta_0$ , and  $A \propto \sqrt{D}$ , in the limit of small transparency,  $D \ll 1$ , extracted from the analytical equations for the MGS spectrum and transition matrix elements [17]. The advantageous property of this analytical model is that it applies to junctions with interface faceting, which is taken into account by average values of the model parameters  $\eta$ ,  $\varepsilon_m$ , and  $\omega_b$ .

Numerical solutions to the modeled Eq. (5) are presented in the inset of Fig. 1. They demonstrate splitting of a single critical point into three critical points at  $\eta = 25$  and  $\omega_b = 3.45\varepsilon_m$ . This phenomenon can be understood as a reentrance effect: At high temperature the thermal activation undergoes a transition to MQT in the absence of interaction with MGS since the MGS are saturated; with lowering temperature, the MQT rate decreases because of increased interaction with MGS, and thermal activation takes over; then it undergoes the second transition to MQT in the presence of interaction. This finding constitutes the first main results of this Letter.

In the experiment with a tilt yttrium barium copper oxide (YBCO) junction [9], an anomalous temperature dependence of the Josephson current decay rate has been observed, which can be interpreted in terms of the reentrance effect: transition to the MQT regime at  $T_1 \approx 135$  mK is interrupted, at  $T_2 \approx 90$  mK, by reentrance of the thermal activation, which then undergoes the second MQT transition at  $T_3 \approx 45$  mK, as sketched in Fig. 1. To make a quantitative comparison we fit the three experimental transition temperatures by adjusting the average model parameter values  $\eta$ ,  $\varepsilon_m$ , and  $\omega_b$  [17], as shown in Fig. 1. Including the stray LC oscillator of the experimental setup [19] does not make any qualitative difference but rather insignificantly (within 20%) shifts the parameters' values. The best fit is eventually achieved for the values  $\varepsilon_m \approx 320$  mK,  $\omega_b \approx 1.7$  K,  $\omega_p \approx 2.5$  K, and  $C \approx 36$  fF, assuming experimental values of the critical current,  $I_C = 1.4 \mu\text{A}$ , and the switching current,  $I_e \approx 0.9I_C$ . Given the experimental junction transparency,  $D \sim 10^{-4}$ , we are able to evaluate the maximum energy gap at the interface,  $\Delta_0 \approx 16$  K.

In our discussion the temperature dependence of the *adiabatic* Josephson potential has been ignored. This dependence, also originating from the thermal saturation of the MGS band, may play a role in junctions with large capacitance where it may modify, as shown in [9], the thermally activated decay rate and provide an alternative explanation to the experimentally observed feature.

Consistency of our *nonadiabatic* reentrance scenario with the experimental observations strongly indicates involvement of the MGS pairs in the macroscopic dynamics of the junction. Moreover, it provides us with valuable information about the microscopic MGS parameters.

*Nonlinear resonance Josephson dynamics.*—To investigate the real time Josephson dynamics, one needs to generalize our approach to nonequilibrium states. This is done by considering the partition function defined through the action on the real time Keldysh contour [20]. Then proceeding as before, by introducing the instantaneous basis, we derive the equation for the Keldysh-Green functions,  $\hat{G}^{ab}$ ,  $[i\partial_t - \hat{H}(\varphi^a, \dot{\varphi}^a)]\hat{G}^{ab}(t-t') = a\delta^{ab}\delta(t-t')$ , with the same Hamiltonian as in Eq. (1); here  $a, b = \pm$  label the forward and backward branches of the Keldysh contour. The semiclassical dynamics of the superconducting phase is given by the least action principle,  $(\delta/\delta\chi)S_{\text{eff}}[\varphi, \chi]_{\chi=0} = 0$ , formulated in terms of the Wigner variables,  $\varphi^a = \varphi + a\chi/2$  [21]. Calculating the functional derivative, we get

$$\frac{C}{2e}\dot{\varphi} + \text{Tr}(\hat{I}_J \hat{\rho}) = I_e. \quad (6)$$

Here  $\hat{\rho}(t) = (1/2i)\sum_a \hat{G}^{aa}(t, t)$  is the nonequilibrium single particle density matrix, which satisfies, by virtue of the equation for  $\hat{G}^{ab}$ , the Liouville equation,

$$i\dot{\hat{\rho}} = [\hat{H}, \hat{\rho}], \quad \hat{H} = \hat{E} - \dot{\varphi} \hat{\mathcal{A}}. \quad (7)$$

Equations (6), (3), and (7) are exact in the semiclassical limit and give a general description of the nonadiabatic Josephson dynamics in all kinds of junctions. These equations constitute another main result of this Letter.

For the MGS pairs, Eq. (7) reduces to the Bloch equation for the two-level density matrix parametrized with the angle  $\theta$ . In this case, Eqs. (6) and (7) become analogous to the ones describing electromagnetic modes in a cavity embedded in a medium of two-level atoms [4]. The most interesting is the case of the resonant excitation of the MGS pairs, which corresponds to the Josephson plasma frequency lying within the MGS band,  $\omega_p < \varepsilon_m$ . Suppose a small oscillating biasing current is applied to the junction,  $I_e \cos \omega t$ , with frequency slightly detuned from the plasma frequency,  $\delta = \omega - \omega_p \ll \omega$ . The resonant dynamics of the superconducting phase,  $\varphi(t) = \text{Re}(\varphi_\omega e^{-i\omega t})$ , is described by the averaged equation for slow varying complex amplitude,  $\varphi_\omega(t)$ ,

$$-2i\dot{\varphi}_\omega + [-2\delta + \gamma(r)]\varphi_\omega = eI_e/\omega_p C, \quad (8)$$

where  $\gamma = \gamma' + i\gamma''$  is the nonlinear MGS response,

$$\gamma'(r) = \gamma'_0 + \partial_\varphi^2 \bar{\varepsilon} \frac{\gamma''}{\Gamma_1} r^2, \quad \gamma''(r) = \frac{\Gamma \gamma''_0}{\sqrt{(r\bar{A}\omega)^2 + \Gamma^2}} \quad (9)$$

[the nonlinear adiabatic term is dropped from Eq. (8) to emphasize the MGS effect]. In Eq. (9) the bar indicates the



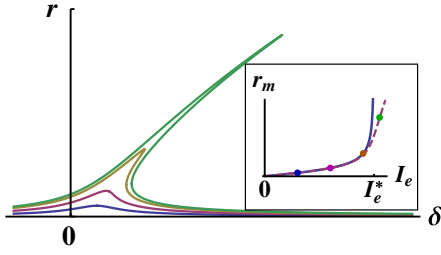


FIG. 2 (color online). Effect of MGS on nonlinear resonance response of the junction. Response amplitude as function of detuning is shown for different amplitudes of driving current. Inset: Maximum response amplitude as a function of driving current, dots indicate current values in the main figure.

resonant values,  $r = |\varphi_\omega|$ , and the quantity  $\gamma_0$  refers to the linear MGS response given by the analytical continuation of Eq. (4) to real frequencies,  $i\nu \rightarrow \omega + i0$ . The response is calculated [17] by solving the Bloch equation (7) assuming the MGS adiabatically following, in the rotating frame, the evolution of the phase amplitude, and adding small decoherence rates  $\Gamma_1, \Gamma_2 \ll \varepsilon_m$ . The MGS decoherence is induced, e.g., by scattering to the itinerant nodal states by the facet edges or other rare inhomogeneities, leading to the MGS intrinsic broadening,  $\Gamma = \sqrt{\Gamma_1 \Gamma_2}$ . The dissipative part of the linear response is estimated,

$$\gamma_0''(\omega, T) \sim \frac{\omega}{\varepsilon_m R_n C} \tanh \frac{\omega}{4T}. \quad (10)$$

It gives the frequency independent quality factor at zero temperature,  $Q_{\text{MGS}} = \omega/\gamma_0'' \sim \varepsilon_m R_n C$ . It is instructive to compare this result to the damping effect of the nodal quasiparticles,  $Q_{\text{nodal}} \sim \Delta_0 R_n C \gg Q_{\text{MGS}}$  [17] (cf. [22–24]).

Equation (9) provides an extension of the linear response equation (4) to the nonlinear region, when the Rabi frequency of MGS transitions exceeds the MGS intrinsic width,  $r\bar{A}\omega \gtrsim \Gamma$ . In this nonlinear regime relevant for narrow MGS levels the stationary response amplitude as a function of detuning is defined by the relation

$$\delta = \frac{1}{2} \gamma'(r) \pm \frac{1}{2r} \sqrt{(eI_e/C\omega_p)^2 - [\gamma''(r)r]^2}. \quad (11)$$

The response demonstrates the bifurcation regime shown in Fig. 2, which is typical for nonlinear oscillators, but here is entirely controlled by MGS characteristics rather than adiabatic Josephson potential. The bifurcation appears at very small driving currents,  $\tilde{I}_e = (I_e/2I_C)Q_{\text{MGS}} \sim \Gamma/\omega\bar{A} \ll 1$ . The most striking feature of the response is the explosive growth of the peak amplitude,  $r_{\text{max}} = \tilde{I}_e [1 - (\tilde{I}_e/I_e^*)^2]^{-1/2}$ , for the driving current approaching the value  $I_e^* = \Gamma/\omega\bar{A}$ . This effect is caused by the MGS saturation at large driving amplitudes, which is manifested by decreasing damping in Eq. (9). The divergency is smeared by adding small damping, e.g., by nodal quasiparticles, and changes to a steep dependence asymptotically approaching the line,  $r_{\text{max}} = (\tilde{I}_e - I_e^*)(Q_{\text{nod}}/Q_{\text{MGS}})$ . The Rabi dynam-

ics of the MGS should be more clearly exposed in the time resolved experiments.

In conclusion, we considered the effects of midgap states on Josephson dynamics in  $d$ -wave superconducting junctions. The analysis is based on the developed general theoretical framework for nonadiabatic Josephson dynamics in junctions containing low energy quasiparticles. We identified a reentrance effect in MQT and connected that to the experimental observations. We also investigated the nonlinear dynamical response of the junction caused by coupling to nonlinear MGS dynamics.

We are thankful to J. Clarke, M. Fogelström, T. Löfwander, and C. Tsuei for useful discussions, and illuminative discussion of experiment with Th. Bauch and F. Lombardi are gratefully acknowledged. The work was supported by the Swedish Research Council (VR) and the European FP7-ICT Project MIDAS.

- 
- [1] Y. Makhlin, G. Schön, and A. Shnirman, *Rev. Mod. Phys.* **73**, 357 (2001).
  - [2] G. Wendin and V. S. Shumeiko, *Low Temp. Phys.* **33**, 724 (2007).
  - [3] J. Clarke and F. K. Wilhelm, *Nature (London)* **453**, 1031 (2008).
  - [4] L. Allen and J. H. Eberly, *Optical Resonance and Two-Level Atoms* (Dover, New York, 1987).
  - [5] H. Hilgkamp and J. Mannhart, *Rev. Mod. Phys.* **74**, 485 (2002).
  - [6] C.-R. Hu, *Phys. Rev. Lett.* **72**, 1526 (1994).
  - [7] D. J. Van Harlingen, *Rev. Mod. Phys.* **67**, 515 (1995).
  - [8] C. C. Tsuei and J. R. Kirtley, *Rev. Mod. Phys.* **72**, 969 (2000).
  - [9] Th. Bauch *et al.*, *Phys. Rev. Lett.* **94**, 087003 (2005).
  - [10] M. Covington *et al.*, *Phys. Rev. Lett.* **79**, 277 (1997).
  - [11] G. Testa *et al.*, *Phys. Rev. B* **71**, 134520 (2005).
  - [12] T. Löfwander, V. S. Shumeiko, and G. Wendin, *Supercond. Sci. Technol.* **14**, R53 (2001).
  - [13] S. Kashiwaya and Y. Tanaka, *Rep. Prog. Phys.* **63**, 1641 (2000).
  - [14] H. Grabert and U. Weiss, *Phys. Rev. Lett.* **53**, 1787 (1984).
  - [15] V. Ambegaokar, U. Eckern, and G. Schön, *Phys. Rev. Lett.* **48**, 1745 (1982).
  - [16] A. Zazunov, V. S. Shumeiko, G. Wendin, and E. N. Bratus', *Phys. Rev. B* **71**, 214505 (2005).
  - [17] See supplementary material at <http://link.aps.org/supplemental/10.1103/PhysRevLett.105.127001> for details.
  - [18] D. J. Scalapino, *Phys. Rep.* **250**, 329 (1995).
  - [19] Th. Bauch *et al.*, *Science* **311**, 57 (2006).
  - [20] A. D. Zaikin and G. Schön, *Phys. Rep.* **198**, 237 (1990).
  - [21] A. Kamenev, [arXiv:cond-mat/0412296v2](http://arxiv.org/abs/cond-mat/0412296v2).
  - [22] C. Bruder, A. van Otterlo, and G. T. Zimanyi, *Phys. Rev. B* **51**, 12 904 (1995).
  - [23] Yu. S. Barash, A. V. Galaktionov, and A. D. Zaikin, *Phys. Rev. B* **52**, 665 (1995).
  - [24] S. Kawabata, S. Kashiwaya, Y. Asano, and Y. Tanaka, *Phys. Rev. B* **72**, 052506 (2005).